The evolution of gamma-ray burst jet opening angle through cosmic time

Monthly Notices
of the
ROYAL ASTRONOMICAL SOCIETY

MNRAS **494,** 4371–4381 (2020)
Advance Access publication 2020 April 21

doi:10.1093/mnras/staa1057

The evolution of gamma-ray burst jet opening angle through cosmic time

Nicole Lloyd-Ronning [1,2★] Valeria U. Hurtado,[1] Aycin Aykutalp,[3] Jarrett Johnson[3] and Chiara Ceccobello [4]

[1]*CCS-2, Los Alamos National Lab, Los Alamos, NM 87544, USA*
[2]*Department of Science and Engineering, University of New Mexico, Los Alamos, NM 87544, USA*
[3]*XTD, Los Alamos National Lab, Los Alamos, NM 87544, USA*
[4]*Chalmers University of Technology, Onsala Space Observatory, SE-439 92 Onsala, Sweden*

Accepted 2020 April 16. Received 2020 April 16; in original form 2019 November 29

ABSTRACT

Jet opening angles of long gamma-ray bursts (lGRBs) appear to evolve in cosmic time, with lGRBs at higher redshifts being on average more narrowly beamed than those at lower redshifts. We examine the nature of this anticorrelation in the context of collimation by the progenitor stellar envelope. First, we show that the data indicate a strong correlation between gamma-ray luminosity and jet opening angle, and suggest this is a natural selection effect – only the most luminous GRBs are able to successfully launch jets with large opening angles. Then, by considering progenitor properties expected to evolve through cosmic time, we show that denser stars lead to more collimated jets; we argue that the apparent anticorrelation between opening angle and redshift can be accounted for if lGRB massive star progenitors at high redshifts have higher average density compared to those at lower redshifts. This may be viable for an evolving initial mass function (IMF) – under the assumption that average density scales directly with mass, this relationship is consistent with the form of the IMF mass evolution suggested in the literature. The jet angle–redshift anticorrelation may also be explained if the lGRB progenitor population is dominated by massive stars at high redshift, while lower redshift lGRBs allow for a greater diversity of progenitor systems (that may fail to collimate the jet as acutely). Overall, however, we find both the jet angle–redshift anticorrelation and jet angle–luminosity correlation are consistent with the conditions of jet launch through, and collimation by, the envelope of a massive star progenitor.

Key words: gamma-ray burst: general.

1 INTRODUCTION

Although we have learned much about gamma-ray bursts (GRBs) over the last 20 yr, there are still a number of open questions related to the nature of their underlying progenitor systems. It is well established that they are associated with the deaths of massive stars and/or merging binary systems (for reviews summarizing the arguments and evidence for this, see Piran 2004; Zhang & Mészáros 2004; Mészáros 2006; Lee & Ramirez-Ruiz 2007; Gehrels, Ramirez-Ruiz & Fox 2009; Berger 2014; D'Avanzo 2015; Levan et al. 2016). However, it is also clear that very special conditions are required to successfully launch a GRB jet. These conditions distill down to the inner engine having enough angular momentum and power to launch a relativistic jet that can propagate through a surrounding hydrogen-stripped envelope.

There are many proposed systems capable of producing a GRB and in reality, probably several (or all) of these systems contribute to the total GRB population. Levan et al. (2016) summarize different progenitor systems for lGRBs, including various single-star and binary formation channels, the rates of these different formation channels, and other important considerations (e.g. host galaxy properties, etc.). Signatures of specific progenitor systems, like locations in their host galaxies (Bloom, Kulkarni & Djorgovski 2002; Fong, Berger & Fox 2010; Fong & Berger 2013; Lyman et al. 2017), or coincident emission associated with a supernova (Galama et al. 1998; Hjorth et al. 2003; Woosley & Bloom 2006; Hjorth & Bloom 2012), kilonova (Metzger et al. 2010; Tanvir et al. 2013; Troja et al. 2018), or the presence of gravitational wave emission (Abbott et al. 2017) can potentially help distinguish among progenitor systems for both long and short GRBs. In addition, there are many correlations present among observed and fitted GRB variables (see e.g. the recent review by Dainotti, Del Vecchio & Tarnopolski 2018), which may help to elucidate the underlying progenitor.

★ E-mail: lloyd-ronning@lanl.gov

In this paper, we consider how different progenitor systems connect to GRB observables over cosmic time. We are motivated by the results of Lloyd-Ronning, Aykutalp & Johnson (2019b) who found that certain intrinsic long gamma-ray burst (lGRB) properties appear to evolve with redshift, even when accounting for Malmquist-type biases and selection effects in the observed data. This and previous studies (Lloyd-Ronning, Fryer & Ramirez-Ruiz 2002; Wei & Gao 2003; Yonetoku et al. 2004; Kocevski & Liang 2006; Petrosian, Kitanidis & Kocevski 2015; Yu et al. 2015; Deng et al. 2016; Tsvetkova et al. 2017; Xue, Zhang & Zhu 2019) have shown that isotropic energy and luminosity evolve as a function of redshift, with lGRBs being brighter at higher redshifts even when accounting for selection effects that favour detecting more luminous bursts at high redshifts. However, in the hundred or so bursts where jet opening angle estimates are available and for which one can compute beaming angle corrected (i.e. actual emitted) gamma-ray energy and luminosity, Lloyd-Ronning et al. (2019b) found these variables (i.e. gamma-ray luminosity and emitted energy) are *not* correlated with redshift. This suggests that jet opening angle *is*, and indeed they found a significant anticorrelation between jet opening angle and redshift. This relationship between jet angle and redshift was suggested in Lloyd-Ronning et al. (2002, see e.g. their section 5.1.2), and observational evidence for this anticorrelation has also been put forth by Yonetoku et al. (2005), Lü et al. (2012), and Laskar et al. (2014, 2018a, b).

If this apparent anticorrelation – with higher redshift lGRBs more narrowly beamed than lower redshift lGRBS – is true, its underlying cause is not clear. Beaming angle evolution over cosmic time could be a reflection of the evolution of any number of properties or processes that affect the lGRB jet – for example, the average stellar density profile, the spin and magnetic field geometry of the central engine, etc. This correlation can also be affected by the degree of sideways spreading of the jet when it breaks free of the star, as well as inherent and observational selection effects.

Our goal in this paper is to understand the potential beaming angle evolution in the context of collimation by the stellar envelope, and how it relates to lGRB progenitor properties. Our paper is organized as follows. In Section 2, we summarize the general properties of different GRB progenitor models. In Section 3, we examine the luminosity requirements both for launching a successful jet and for collimation by the stellar envelope. We show there is a strong correlation between emitted gamma-ray luminosity and jet opening angle, and suggest this is a natural selection effect where only the more luminous lGRBs can launch wider opening angle jets. In Section 4, we discuss collimation of the jet by a massive star envelope and how evolution of certain intrinsic properties such as mass and metallicity can lead to the evolution of the jet opening angle. In particular, we show that the beaming angle–redshift anticorrelation can be explained if high-redshift lGRB progenitors are denser compared to those at lower redshift, which may be expected for an evolving initial mass function (IMF). In Section 5, we present a summary and our conclusions.

2 DATA SAMPLE AND SELECTION EFFECTS

Our data are taken from Wang et al. (2020), who compiled publicly available observations and fitted GRB parameters for 6289 GRBs from 1991 to 2016. This data sample contains all previously published jet opening angle estimates (each entry in their electronically available table gives the reference where they obtained the data point), with a total of 137 lGRBs for which these data are available. These jet opening angles are determined from a break (specifically, a steepening) at a given point in time in the afterglow (X-ray, optical, and/or radio) light curve; the time of the break reflects when the forward blast wave has decelerated to a point at which the relativistic beaming of the radiation is comparable to the physical jet opening angle (Rhoads 1999). Although this is a well-established and widely accepted method to get a reasonable estimate of the GRB jet opening angle, these methods rely on assumptions about the GRB outflow and jet structure, as well as its external density profile. We discuss the physical nature and potential uncertainties in the jet opening angle estimates further in Section 5.

2.1 Statistical analysis of the correlation

In Lloyd-Ronning et al. (2019b), we found an anticorrelation between beaming angle and redshift that can be parametrized as $\theta_j \propto (1+z)^{-0.75\pm0.25}$. In that paper, we use well-established non-parametric techniques (Lynden-Bell 1971; Efron & Petrosian 1992) to account for Malmquist biases in the detection of high-redshift GRBs. To estimate the significance of the correlation, we use additional non-parametric rank-order correlation tests (such as Kendell's τ and Spearman rank; for a nice explanation of these tests, see e.g. Press et al. 2007). These types of statistical tests are useful because there are no assumptions about the underlying distributions of the variables being evaluated. However, they have other drawbacks – in particular, they do not easily account for measurement error (see e.g. Kitagawa, Nybom & Stuhler 2018). There are techniques developed to estimate correlations accounting for measurement error (Kelly 2007), and these are particularly powerful when the error dominates the scatter in the data. However, these techniques again rely on making some assumptions (however reasonable) about the underlying distributions of the variables and their errors. In our case, because the scatter in the data is larger than the data points' error bars, we do not expect that the presence of measurement error will significantly affect the correlation. To test this statement, however, we performed a series of simulations in which we drew each data point from a uniform distribution within in its 1σ error bars. In all cases, we still found an anticorrelation between θ_j and $(1+z)$ to high statistical significance.

For the purposes of this study, the results of the rank correlation tests provide a fairly robust method of estimating the probability of a correlation in the data. However, the presence of observational selection effects can in some cases lead to false (statistically significant) correlations in the data. We discuss this important point in the following section.

2.2 The role of selection effects

Before discussing the potential physical nature of jet opening angle evolution, it is important to consider whether selection effects may be playing a role in producing the apparent relationship. For example, Lü et al. (2012) found a similar statistically significant correlation between jet opening angle and redshift in their sample of 77 lGRBS, with $\theta_j \propto (1+z)^{-0.94\pm0.19}$. They argue, however, that the correlation can be explained by observational biases. Their analysis relies on having to assume specific functional forms for their underlying variables, including the lGRB rate density, luminosity function, jet beaming angle distribution, and additional assumptions about the detector response rate. Importantly, they have assumed that the lGRB rate density follows the star formation rate, a conjecture that has been called into question by a number of studies, based on lGRB observations (e.g. Lloyd-Ronning et al. 2002; Kistler et al. 2008; Yüksel et al. 2008; Kistler et al. 2009;

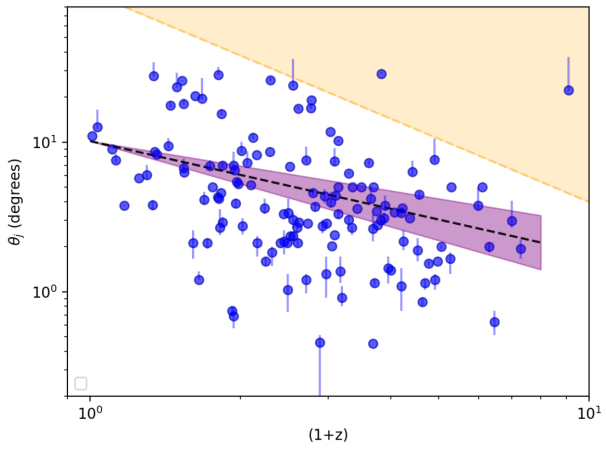

Figure 1. Jet opening angle versus redshift. The dashed black line and purple region show the best fit to the data, $\theta_j \propto (1+z)^{-0.75 \pm 0.25}$. The orange shaded area indicates a region of possible selection bias.

Petrosian et al. 2015; Lloyd-Ronning et al. 2019b). Because of the degeneracy among the physical variables and the lack of knowledge of their true underlying distributions, it is difficult to draw definitive conclusions about the role of selection effects through this approach. As we discuss below, non-parametric techniques developed to deal with fairly well-defined selection criteria can be a useful tool to determining the true correlation between variables (Lynden-Bell 1971; Efron & Petrosian 1992). To do so, however, we need to get a handle on what these selection effects are.

As discussed in the introduction, many of the issues related to Malmquist-like selection effects in this sample have been addressed in Lloyd-Ronning et al. (2019b). However, it is important to ask how missing a fraction of low(er) luminosity GRBs at high redshift due to detector sensitivity limits might affect our results. Such a selection effect would lead to a corresponding lack of lower luminosity, smaller jet angle data points (because jet angle is correlated with luminosity; see Lü et al. 2012 and Section 4). Therefore, adding these data points to our sample – if indeed they are there and we are simply not seeing them – would strengthen the anticorrelation between jet opening angle and redshift. That is, because luminosity is correlated with jet opening angle, missed low-luminosity GRBs at high redshift would have on average smaller opening angles. Adding such GRBs to our sample would then place more small opening angle GRBs at high redshift, strengthening our correlation.

However, another important possibility is that we are missing a fraction of larger opening angle GRBs at high redshift, because the jet break occurs too late in the afterglow light curve to be detected (i.e. the afterglow light curve has faded below detector limits before the jet break can be detected). There are a couple of things that mitigate this effect, however. First, lGRBs are not standard candles so the intrinsic scatter in their afterglow luminosities helps soften this effect to some extent. Additionally, lGRBs with larger opening angles should have larger average luminosities, and are less likely to be missed by the detector (relative to low-luminosity lGRBs); therefore we suggest this effect may not be playing a significant role in artificially producing a $\theta_j - (1+z)$ anticorrelation.

To examine the severity and effect of this latter potential bias, we have produced a strong truncation in the $\theta_j - (1+z)$ plane, in which larger jet opening angles at high redshift are missed due to observational selection effects. This is shown by the orange shaded region in Fig. 1 (note this region excludes a couple of observed lGRBs, and so is potentially more severe than necessary). Applying this truncation to our sample and performing the rank statistics discussed in Lynden-Bell (1971) and Efron & Petrosian (1992), we still find a significant anticorrelation between θ_j and $(1+z)$. Again, we favour the non-parametric approach in determining the significance of the correlation between variables because we do not need to make assumptions about the parent population distributions, and they have been shown to reveal true underlying correlations very well. For example, the appendix of Lloyd, Petrosian & Mallozzi (2000) demonstrates how powerful these methods can be in recovering the underlying distributions of relevant variables (and the correlation between them) in the presence of truncation. In their Figs 7 and 8, they show simulations of two important cases: (1) when the truncation produces an artificial correlation, and (2) when the truncation removes a true, underlying correlation. In both cases, applying the methods of Lynden-Bell (1971) and Efron & Petrosian (1992) reproduces the true, underlying distributions of, and correlations among, the variables at hand. Other methods to incorporate selection effects based on a Bayes approach are described in Mandel, Farr & Gair (2019) (and although powerful, these methods do rely on making some assumptions about the underlying distributions of the variables).

There are a variety of approaches one can employ to deal with complicated observational selection effects. In Lloyd-Ronning et al. (2019b) (where we initially report this correlation) and in this paper, we have chosen to use well-established non-parametric rank-order techniques because – again – they do not require assumptions about the underlying distributions of the variables being analysed. The complexity of this issue, however, may leave some room to question the presence of a physical anticorrelation between θ_j and $(1+z)$. We emphasize that the purpose of this paper is to explore a possible physical interpretation behind this potential correlation. In other words, as we show below, we *predict* such an anticorrelation between lGRB beaming angle and redshift should exist if stars in the early Universe are more massive (on average) and/or have lower metallicity than stars at lower redshift.

3 PROGENITOR MODELS

As mentioned in the introduction, there are several general requirements that appear necessary to produce a successful relativistic GRB jet. These include: (1) enough mass and angular momentum in the system to sustain an accretion disc and launch a jet; (2) no hydrogen envelope; this is based on both theory (the requirement that the jet is able to breakout from the system's envelope) and observations of Type Ic supernova associated with lGRBs; and (3) significant magnetic flux (along with angular momentum) to launch a jet [assuming a magnetically launched jet as in the Blandford–Znajek framework (Blandford & Znajek 1977); see e.g. Barkov & Komissarov 2008; Komissarov & Barkov 2009; Barkov & Komissarov 2010; Lloyd-Ronning et al. 2019a for a consideration of these conditions for lGRB systems]. We discuss these requirements briefly and generally in the context of several of lGRB progenitor systems.

3.1 Single massive star progenitors

A number of studies have shown the viability of a massive star progenitor for lGRBs from a theoretical point of view (e.g. Woosley 1993; MacFadyen & Woosley 1999; Woosley & Heger 2006; Kumar, Narayan & Johnson 2008a, b; and recently Obergaulinger & Aloy 2020). In addition, there is strong observational evidence, both

through supernova associations (see e.g. Hjorth & Bloom 2012) and locations in star-forming regions in their host galaxies (Bloom et al. 2002; Lyman et al. 2017) that lGRBs are associated with the deaths of massive stars. [We note there are two examples (GRB060505 and GRB060614, which lie in the in-between ground of lGRB and sGRB in terms of duration) that do *not* have associated SNe to deep limits (Della Valle et al. 2006; Fynbo et al. 2006; Gal-Yam et al. 2006; Gehrels et al. 2006)].

How a collapsing star loses its hydrogen envelope and retains the angular momentum to sustain a disc and launch a jet is a complicated question. Stars with higher metallicity are particularly problematic because the associated mass-loss carries angular momentum. Lower metallicity stars may be more viable candidates, since mass-loss goes roughly as $Z^{0.7-0.8}$, where Z is metallicity (Vink, de Koter & Lamers 2001; Vink & de Koter 2005). If one has a low metallicity star therefore one might expect the necessary angular momentum can be retained, and indeed this is one of the motivations behind considering Population III stars as GRB progenitors (Bromm & Loeb 2006; Suwa & Ioka 2011; Yoon, Dierks & Langer 2012). However, other factors such as torques from magnetic fields and/or other coupling between the elemental layers of stars can cause a loss of the necessary angular momentum. Chemically homogeneous evolution helps mitigate the latter effect. This is addressed in Woosley & Heger (2006), who assert about 1 per cent of stars can achieve the conditions needed to retain enough angular momentum to launch a GRB (keep in mind that their models are one dimensional and asymmetric mass-loss may help, allowing for less angular momentum loss). However, this process needs to occur during the early stages of a star and – again – is more efficient for lower metallicity stars (further discussion of these issues can also be found in section 5.2 of Levan et al. 2016).

Although massive stars can span a range of mass and metallicities, and can meet the energy and time-scale requirements for an lGRB, the difficulties associated with retaining enough angular momentum are one of the motivations for considering binary formation channels for lGRBs.

3.2 Binary formation channels

Binary systems are thought to make up at least half of the massive stars (Kobulnicky et al. 2014). As with single massive star progenitors, binary lGRB progenitors need to strip the hydrogen envelope and retain enough mass and angular momentum to allow for GRB jet launch. The advantage to binary progenitors is that the conditions of hydrogen envelope stripping and high angular momentum are in principle readily met, due to the interaction with the companion star (Belczynski, Bulik & Rudak 2002; Fryer & Heger 2005; Davies et al. 2007; Barkov & Komissarov 2010; de Mink et al. 2013; Levan et al. 2016; Kinugawa & Asano 2017; Chrimes, Stanway & Eldridge 2020)

Viable binary progenitors for lGRBs include:

(i) *Helium mergers* (Fryer & Woosley 1998; Zhang & Fryer 2001; Fryer et al. 2013). In this model, a compact object merges with the helium core of an evolved companion. In the process, the hydrogen envelope is ejected and the compact object is spun up so that the conditions for launching an lGRB jet are met. This model can achieve the necessary energetics and time-scales to be a viable lGRB progenitor.

(ii) *CO core mergers*. A related model is the so-called binary-driven hypernova involving accretion induced collapse (for a recent summary of this model see Rueda, Ruffini & Wang 2019). In this scenario, a carbon–oxygen core undergoes a supernova which causes rapid accretion on to a neutron star companion. Similar to the He-merger model, it can achieve the conditions required to launch a relativistic GRB jet.

(iii) *White dwarf–black hole/NS binaries* (King, Olsson & Davies 2007). In this model, a white dwarf merges with a black hole or neutron star companion and can produce an lGRB, in some cases without an accompanying supernova.

(iv) *Micro-TDEs* (Perets et al. 2016). In this model a neutron star or black hole tidally disrupts a star, leading to a debris disc around the compact object that can launch a relativistic jet. This model was initially proposed to explain ultra-long GRBs, but may contribute to the standard lGRB population.

Other binary systems not considered here (e.g. Cantiello et al. 2007; Callingham et al. 2019) may also contribute to the lGRB population. Because of the vast array of binary systems, their formation channels and subsequent evolution, they may span a range of masses/energies, metallicities, angular momenta, and have a range of different ambient environments. We note that some simulations (e.g. Yoon, Woosley & Langer 2010) of binary progenitors for lGRBs – particularly those able to produce Type Ic SNe – find in fact not enough angular momentum is retained to launch an lGRB. As with massive star progenitors, however, lower metallicity conditions in these systems may help (Kinugawa & Asano 2017), as well as a stage of chemically homogeneous evolution (see e.g. the recent discussion in Chrimes et al. 2020).

3.3 Expected cosmological evolution of GRB intrinsic and environmental properties

The primary properties of lGRB progenitors expected to evolve through cosmic time are stellar mass and metallicity (which are of course themselves related). Metallicity evolves with redshift (i.e. Vink et al. 2001; Vink & de Koter 2005) as stars in the early Universe have not had the time to synthesize a large amount of metals. A star's metallicity can affect its mass, spin, and stellar density profile. For example, the distribution of zero-age main-sequence stellar masses is expected to evolve over cosmic time largely as a result of lower metallicity conditions allowing more massive stars to form (Kroupa 2019). Evidence for the evolution of this IMF has been suggested by a number of authors (e.g. van Dokkum & van der Marel 2007; Davé 2008; Wang & Dai 2011; Marks et al. 2012; and more recently Leja et al. 2020; Chruslinska et al. 2020). Overall stellar mass can affect the lGRB energy budget and – as we discuss below – the stellar density profile, where more massive stars may serve to collimate a jet more effectively.

4 LUMINOSITY REQUIREMENTS FOR SUCCESSFUL JET LAUNCH AND COLLIMATION

It takes a certain amount of power in order for a jet to borough through a stellar envelope (although there may exist a pre-jet that evacuates the polar region, easing this requirement, e.g. Burrows et al. 2007). A key quantity that needs to be considered is the ratio of the jet energy density to ambient medium energy density, given by (Matzner 2003; Bromberg et al. 2011; Hamidani, Kiuchi & Ioka 2020)

$$\widetilde{L} = \frac{\rho_{\rm j}\eta_{\rm j}\Gamma_{\rm j}^2}{\rho_{\rm a}\eta_{\rm a}\Gamma_{\rm a}^2}, \quad (1)$$

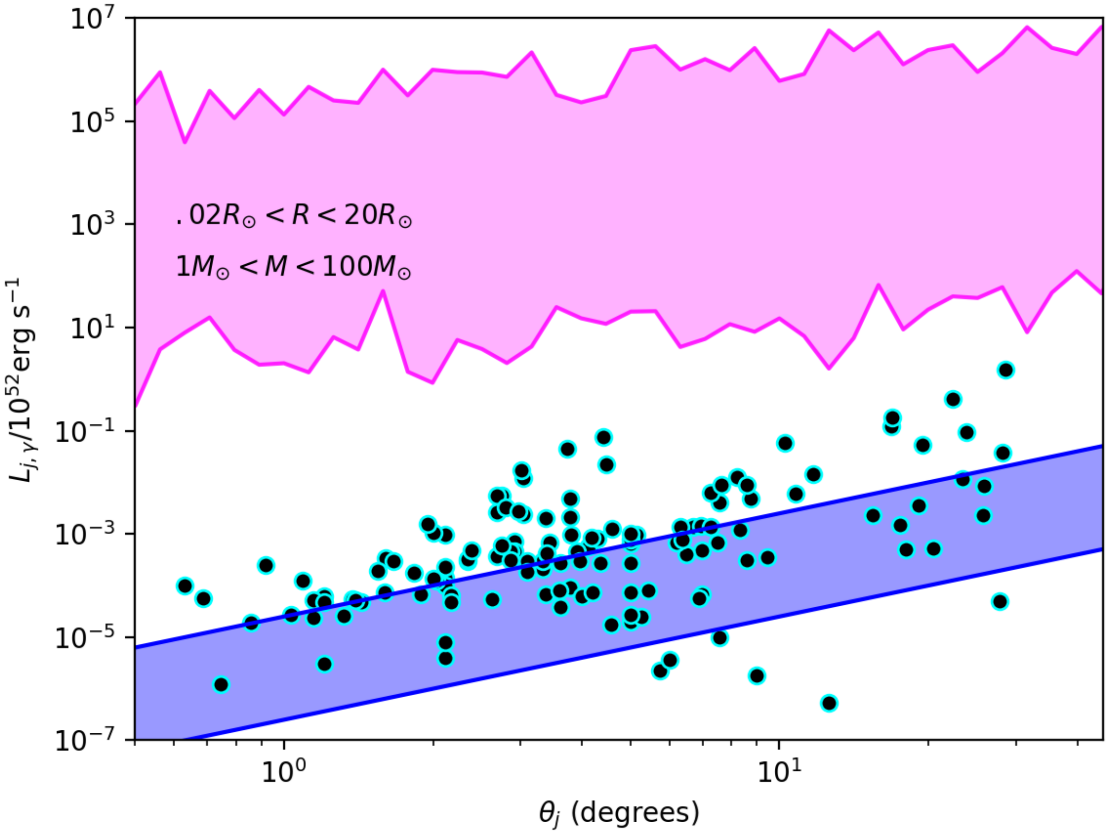

Figure 2. Gamma-ray luminosity versus jet opening angle. The upper magenta band shows the upper limit to the jet luminosity required to ensure a collimated jet (Matzner 2003; Bromberg et al. 2011) for extreme ranges of mass and progenitor stellar radii. The fluctuations are due to a random selection of stellar density profile indices ranging from $-3.0 < \alpha < -2.1$, where $\rho \propto r^{-\alpha}$. The lower blue band is the luminosity needed to launch a jet (Aloy, Cuesta-Martínez & Obergaulinger 2018) given a jet injection radius of $h_o = 2 \times 10^9$ cm and an ambient pressure of 1.8×10^{23} erg cm^{-3}, representative of a 35 $M_\odot$ zero-age main-sequence star with enough angular momentum to launch a GRB (Woosley & Heger 2006; Aloy et al. 2018). The blue band spans a gamma-ray efficiency (converting jet power to radiation) of 0.1 per cent to 10 per cent.

where ρ denotes density, η denotes the specific enthalpy, and Γ denotes the Lorentz factor. The subscript j refers to the jet while a refers to the ambient medium. For a static ambient medium $\Gamma_a = 1$ and $\eta_a = 1$.

Given this ratio and the requirement that – as discussed in Aloy et al. (2018) – the outflow must be supersonic with respect to the external medium, there is a requirement on the minimum power a jet must have to launch successfully (Aloy et al. 2018):

$$L_j \gtrsim 10^{49}\mathrm{erg\,s^{-1}} \left(\frac{h}{2x10^9\ \mathrm{cm}}\right)\left(\frac{\theta_j}{2^\circ}\right)\left(\frac{p_a}{1.8x10^{22}\ \mathrm{erg\,cm^{-3}}}\right), \quad (2)$$

where h is the height of the jet, θ_j is the jet opening angle, and p_a is the pressure in the ambient medium.

As shown in Matzner (2003) and Bromberg et al. (2011), there is also an upper limit to the luminosity to ensure the jet is collimated in the stellar envelope. The condition for collimation is given by (Matzner 2003; Bromberg et al. 2011)

$$\widetilde{L} < \theta_o^{-4/3}, \quad (3)$$

where θ_o is the initial jet opening angle. For $\eta_a, \Gamma_a = 1$, this condition becomes

$$\widetilde{L} = \frac{\rho_j \eta_j \Gamma_j^2}{\rho_a} \sim \frac{L_j}{\Sigma_j \rho_a c^3} < \theta_o^{-4/3}, \quad (4)$$

where Σ is the cross-sectional area of the jet. Clearly a key parameter is the stellar density profile, which we expect to go roughly as $\rho_a \sim r^{-3}$ (Matzner & McKee 1999), and this is indeed borne out by numerical simulations of massive stars (Woosley & Heger 2006; Mizuta & Aloy 2009). Chemically homogeneous mixing can affect this profile, however (Woosley & Heger 2006), and it has been shown that, more generally, massive star density profiles go as $\rho \propto r^{-n}$, with n between about 2 and 3 (Matzner & McKee 1999) out to the radius of the helium envelope, with a sharp drop off thereafter. The steepness of the drop off is strongly dependent on the mass-loss/metallicity, with low metallicity stars dropping off more drastically (Woosley & Heger 2006; Mizuta & Aloy 2009; Suwa & Ioka 2011). Following Bromberg et al. (2011), we write the ambient density as $\rho_a = \overline{\rho}(h/R)^{-\alpha}$; the parameter $\overline{\rho} = ((3-\alpha)/4\pi)MR^{-3}$ is the average stellar density, where M is the mass of the star and R is the stellar radius.

Then, the condition from equation (4) above can be written as (Bromberg et al. 2011)

$$L_j < 10^{54}\,\mathrm{erg\,s^{-1}} \left(\frac{R}{R_\odot}\right)^{-1}\left(\frac{h}{R}\right)^{2-\alpha}\left(\frac{\theta_o}{10^\circ}\right)^{2/3}\left(\frac{M}{10\,M_\odot}\right). \quad (5)$$

These luminosity conditions for jet launch and collimation (i.e. equations 2 and 5) are shown in Fig. 2 along with the data (gamma-ray luminosity, L_γ, versus measured jet opening angle; black–cyan dots). The upper pink band shows the collimation condition (equation 5) – the upper limit to the luminosity for a mass range and radius range of $0.02R_\odot < R < 20R_\odot$ and $M_\odot < M < 100\ M_\odot$.

The fluctuations reflect a random selection of stellar density profile indices ranging from $-3.0 < \alpha < -2.1$. The lower blue band shows the minimum luminosity (equation 2) needed to launch a jet (Aloy et al. 2018) given a jet injection radius of $R_j = 2 \times 10^9$ cm and an ambient pressure of 1.8×10^{23} erg cm^{-3}, representative of a 35 $M_\odot$ zero-age main-sequence star (Woosley & Heger 2006; Aloy et al. 2018). The band spans a gamma-ray efficiency (converting jet power to radiation) from 0.1 per cent to 10 per cent.

4.1 On the observed correlation between luminosity and jet opening angle

There is a strong correlation between gamma-ray luminosity and measured jet opening angle. The best-fitting line to this correlation is $L_\gamma \propto \theta_j^{1.5\pm0.2}$. Note that the data points that fall below the minimum jet luminosity requirement (blue band in Fig. 2) do not necessarily violate the minimum luminosity requirement – they may simply be indicating a lower efficiency of conversion from jet power to gamma-ray luminosity than we have assumed (1 per cent). That is, the emitted luminosity is only a fraction of the jet energy, $L_\gamma = \epsilon L_j$, and this fraction may lower than 1 per cent for some lGRBs. It is also possible, however, that these GRB progenitors have a smaller envelope pressure than we have assumed (1.8×10^{21} erg cm$^{-3} < p_a < 1.8 \times 10^{23}$ erg cm^{-3}). Either one of these possibilities, however, may say something about the progenitor and/or its environment.

Remembering the pressure in the jet scales as L_j/θ_j^2 and the minimum luminosity to launch a jet scales as θ_j, we can speculate that this correlation arises naturally in a massive star progenitor scenario. Successfully launched jets may sit at a base value of the pressure balance condition (otherwise they may be swallowed by their cocoons), but necessarily satisfying the minimum luminosity condition. The location of the data points in Fig. 2 seems to suggest the jet launch condition plays a larger role in producing this correlation. Ultimately, then, this correlation reflects the successful jet launch condition – only jets with high luminosities can have wide opening angles. This correlation might also be explained if those lGRBs with higher luminosity have higher internal energy in the jet and undergo more sideways expansion such that a wider jet is measured at the time of the afterglow 'jet break' (we discuss this further below).

5 BEAMING ANGLE COLLIMATION AND EVOLUTION

If the anticorrelation between beaming angle and redshift is indeed physical, we would like to understand what determines the observed jet opening angle and how it could evolve through cosmic time – i.e. its relationship to fundamental progenitor properties. Besides the observational selection effects discussed in Section 2, there are a number of issues to consider when attempting to understand the nature of the jet opening angle:

(i) How does the jet launching mechanism affect the initial jet opening angle? For example, in a Blandford–Znajek framework, one should consider how the spin of the black hole and magnetic field strength and geometry serve to constrain the angle of the outflow. Naively, for example, one might expect a higher black hole spin could serve to wind the magnetic field more tightly and lead to a more collimated jet. If lGRB progenitors in the early Universe produce on average more highly spinning black holes or have some property of their magnetic fields that leads to more collimated jets, this could play a role in the beaming angle evolution.

(ii) How the stellar density profile and jet cocoon (Ramirez-Ruiz, Celotti & Rees 2002) structure will serve to collimate the jet.

(iii) The sideways expansion of the jet once it breaks out of the star.

(iv) How the angular structure of the jet plays a role in estimates of the jet opening angle.

The first issue is a complicated question and is perhaps best investigated with detailed general relativistic magneto-hydrodynamic (GRMHD) simulations of black hole–disc–jet systems (Hurtado et al., in preparation). Our focus in this paper is on the second issue. However, we briefly address the third and fourth issues below.

On sideways expansion: It is important to consider what the inferred lGRB beaming angle actually reflects. When the outflow velocity of the jet is decelerated to a point where relativistic beaming ($\sim 1/\Gamma$) is of the order of the physical jet opening angle θ_j, photons are able to escape 'sideways' and a steepening of the light curve will occur (Rhoads 1997, 1999). For a uniform jet, the temporal behaviour of the jet Lorentz factor decelerating in a constant medium is $\Gamma(t) \propto (E/n)^{1/8} t^{-3/8}$, so that $\theta_j \propto (E/n)^{-1/8} t_b^{3/8}$, where t_b is the time of the jet break. Therefore, a break in the afterglow light curve gives an estimate of the jet solid angle at the time of this observed jet break. If the jet has undergone significant sideways expansion, then this opening angle is not an accurate reflection of the true opening angle of the jet as it emerged from the star/progenitor.

Several numerical simulations have examined this problem and shown that the jet does in fact *not* undergo significant sideways expansion, so that it is not unreasonable to take the opening angle at breakout to be the asymptotic jet angle (Mizuta & Aloy 2009; Tchekhovskoy, Narayan & McKinney 2010; Aloy et al. 2018). In other words, in many cases the jet is 'ballistic' and the estimated jet opening angle can be considered a decent estimate of the true jet opening angle.

However, Zhang, Woosley & MacFadyen (2003) find a jet can undergo some amount of sideways expansion when it emerges from the stellar envelope if it has high enough internal energy. In addition, Morsony, Lazzati & Begelman (2007) run FLASH simulations of GRB jets propagating through stars. In particular, they consider a star of low metallicity (1 per cent solar), with an initial mass of 16 $M_\odot$, a final mass of 13.95 $M_\odot$ and a final radius of 4×10^{10} cm. They use a stellar density profile of $\rho \propto r^{-2.5}$ and an equation of state of $p = p_o \rho^{4/3}$ (i.e. ultrarelativistic), ensuring pressure in the star is small compared to ρc^2. They find the jet goes through three phases – a wide opening angle precursor phase, a shocked phase with a narrow opening angle (while in the stellar envelope, being collimated by the stellar envelope), and then an unshocked phase where the jet opening angle increases logarithmically in time (after break out). Finally, Tchekhovskoy et al. (2010) found, using GRBHMD simulations of magnetically launched jets that achieve the necessary (observational) constraint of $\theta_j \Gamma \sim 20$, that – except during an initial short acceleration phase – their jets show little sideways expansion after breakout.

In what follows, we assume the measured opening angle at the time of the break in the afterglow light curve is a decent approximation of the opening angle at breakout (or at least scales with the opening angle at breakout in a uniform way among all GRBs).

On angular energy distribution versus jet 'opening angle': Another thing to keep in mind when considering jet 'opening angle', is the angular energy distribution in the jet. This point is addressed in detail in Mizuta & Aloy (2009), who examine this distribution,

dE/dΩ, for different stellar envelope models (taken from Woosley & Heger 2006). Assuming the same mass, momentum, and energy fluxes for all of their models, they find that the angular energy distribution decays more steeply for lower mass progenitors than high-mass ones. This is because, they argue, the average density of the progenitor grows approximately with mass, and as the mass (density) of the progenitor increases it leads to a slower jet propagation speed inside the star. They suggest that jet slower speed allows for thicker, hotter cocoons to develop and therefore a broader range of dE/dΩ. In what follows below, we assume a relatively steep angular decay for the jet energy distribution so that the 'opening angle' refers to the angle in which most of the jet energy is concentrated.

5.1 Jet collimation by the stellar envelope

There are a number of factors that come into play when considering whether a jet is collimated by its stellar envelope/cocoon system. These are discussed in detail in Matzner (2003) and Bromberg et al. (2011) among others. As discussed in Section 3, these works address the necessary conditions for collimation as a jet propagates through a stellar envelope and forms a cocoon (which ultimately serves to collimate the jet, Ramirez-Ruiz et al. 2002). Their analytic estimates consider mildly to non-relativistic jet heads – as Bromberg et al. (2011) points out, if the head velocity exceeds a certain limit, the cocoon pressure will be too low to collimate it (as they show, this occurs when $L_{\rm j}/(h^2\rho_{\rm a}c^3) \approx \theta_{\rm o}^{5/3}$). This corresponds to a jet head Lorentz factor of $\Gamma_{\rm h} \approx \theta_{\rm o}^{-1/3}$, which is at most mildly relativistic.

Numerical simulations that examine the extent of collimation can be found in Zhang et al. (2003), Mizuta et al. (2006), Morsony et al. (2007), and Tchekhovskoy et al. (2010), all with similar general trends. Zhang et al. (2003) find a jet with an initial half opening angle of 20° propagating through a low metallicity massive star emerges with an opening angle of about 5°. Tchekhovskoy et al. (2010) suggest a relationship between the jet opening angle and stellar radius based on their GRMHD simulations of magnetically launched jets. In particular, they find the scaling $\theta_j \propto (1/R)^{0.22}$. However, we caution that this relationship could arise by design from the way they defined the wall of their jet as input (e.g. their equation 1). Finally, we note that Nagakura et al. (2014) and Hamidani et al. (2020) have examined this problem in the case of a DNS merger scenario. They also find significant jet collimation by the ejecta from the merger. The latter in particular consider the ejecta velocity and its effect on collimation (see their appendix C). These results suggest a general trend toward greater collimation, the longer the jet remains in the star (provided the envelope–cocoon system has enough pressure to collimate).

We would like to get a basic intuition about the extent of the jet collimation by the stellar envelope, and understand how it compares in the context of different progenitor scenarios. There are several ways to approach this but as a first step we can simply compare estimates of the energy densities in the cocoon and jet. The cocoon pressure can be estimated by $p_{\rm c} = \rho_{\rm a}(\beta_{\rm c}c)^2$, where $\beta_{\rm c}$ is the velocity of the cocoon; the jet energy density is given by $L_{\rm j}/(\Sigma_{\rm j}c)$, where $\Sigma_{\rm j} \sim \pi\theta_{\rm j}^2h^2$ is the jet cross-sectional area. In that case, we find the jet opening angle scales as

$$\theta_{\rm j} \propto L_{\rm j}^{1/2}\rho_{\rm a}^{-1/2}h^{-1}. \tag{6}$$

Again, a key parameter in understanding the jet collimation is the stellar density profile. Given that $\rho_{\rm a} = \bar{\rho}(h/R)^{-\alpha}$ (Matzner & McKee 1999), where $2 \lesssim \alpha \lesssim 3$, $\bar{\rho}$ is the average stellar density, and considering the jet angle at breakout (i.e. $h = R$), we find

$$\theta_{\rm j} \propto \left(\frac{L_{\rm j}}{\bar{\rho}R^2}\right)^{1/2}. \tag{7}$$

We can also use the formalism of Morsony et al. (2007) to estimate the degree of jet collimation as it travels through a stellar envelope. Considering the ram pressure due to the deflection of a jet by the boundary layer, and under the condition of a narrow, relativistic jet, they arrive at an expression for the jet opening angle as it propagates through the star:

$$\theta_{\rm j} = \frac{2\theta_{\rm o}}{2 + K\theta_{\rm o}\left(h^2 - h_{\rm o}^2\right)}, \tag{8}$$

where $K = c\pi p_{\rm c}/L_{\rm j}$, h is the height or distance from the jet launch radius and $h_{\rm o}$ is the initial height of jet launch (note they use the variables z and $z_{\rm o}$), and $\theta_{\rm o}$ is the initial jet opening angle (at height $h_{\rm o}$). This equation indicates, as expected, that the farther the jet has to travel through the star, the more it is collimated. If we consider $h \sim R >> h_{\rm o}$ and $K\theta_{\rm o}R^2 >> 2$, then we find

$$\theta_{\rm j} \propto \left(\frac{L_{\rm j}}{\bar{\rho}R^2}\right). \tag{9}$$

This gives a stronger dependence on average density compared to our simple comparison of energy densities (equation 7). None the less, as with equation (7), it points to the direct relationship between jet luminosity and opening angle (as discussed in Section 3) and the inverse relationship between average ambient density and jet opening angle – i.e. that denser stars collimate jets more. In what follows, we focus on $\theta_{\rm j} \propto (1/\bar{\rho})^{1/2}$, but we stress the qualitative behaviour and results remain the same whether we use equation (7) or the stronger dependence in equation (9).

5.2 Cosmological evolution of jet opening angle

Given equation (7) (or 9) above, we can ask whether the jet opening angle dependence on $L_{\rm j}$, $\bar{\rho}$, and/or R might lead to cosmological evolution of this quantity. We have already shown (Lloyd-Ronning et al. 2019b) that the gamma-ray emitted luminosity $L_\gamma (\propto L_{\rm j})$ is not correlated with redshift. Average density, however, is expected to evolve as both the IMF and metallicity evolve throughout cosmic time. We can estimate how the average density, $\bar{\rho} \sim M/R^3$, changes with progenitor properties (e.g. mass, radius, metallicity), and how these quantities are interrelated. Massive main-sequence stars follow a mass–radius relation $R \propto M^{\sim 0.6-0.8}$ (Demircan & Kahraman 1991), although a number of things can complicate this question, like the presence of convection, magnetic fields, etc. Therefore, numerical models of massive stars can be used to estimate the average density for various progenitors. Mizuta & Aloy (2009) have done this and show – using the models of Woosley & Heger (2006) – that the average stellar density for massive stars scales roughly as the stellar mass.

In that case (i.e. assuming average density scales roughly as mass and depends only weakly on radius) we find

$$\theta_{\rm j} \propto [L_{\rm j}/M]^{1/2}. \tag{10}$$

This suggests that *progenitor mass evolution could be the underlying cause of lGRB beaming angle evolution*. Consider the effects of an evolving IMF as suggested in van Dokkum & van der Marel (2007), Davé (2008), Wang & Dai (2011), Marks et al. (2012) and others, and recently Leja et al. (2020), who discuss evidence for a top-heavier IMF at higher redshifts. If average stellar density is indeed roughly proportional to stellar mass for high-mass stars, then

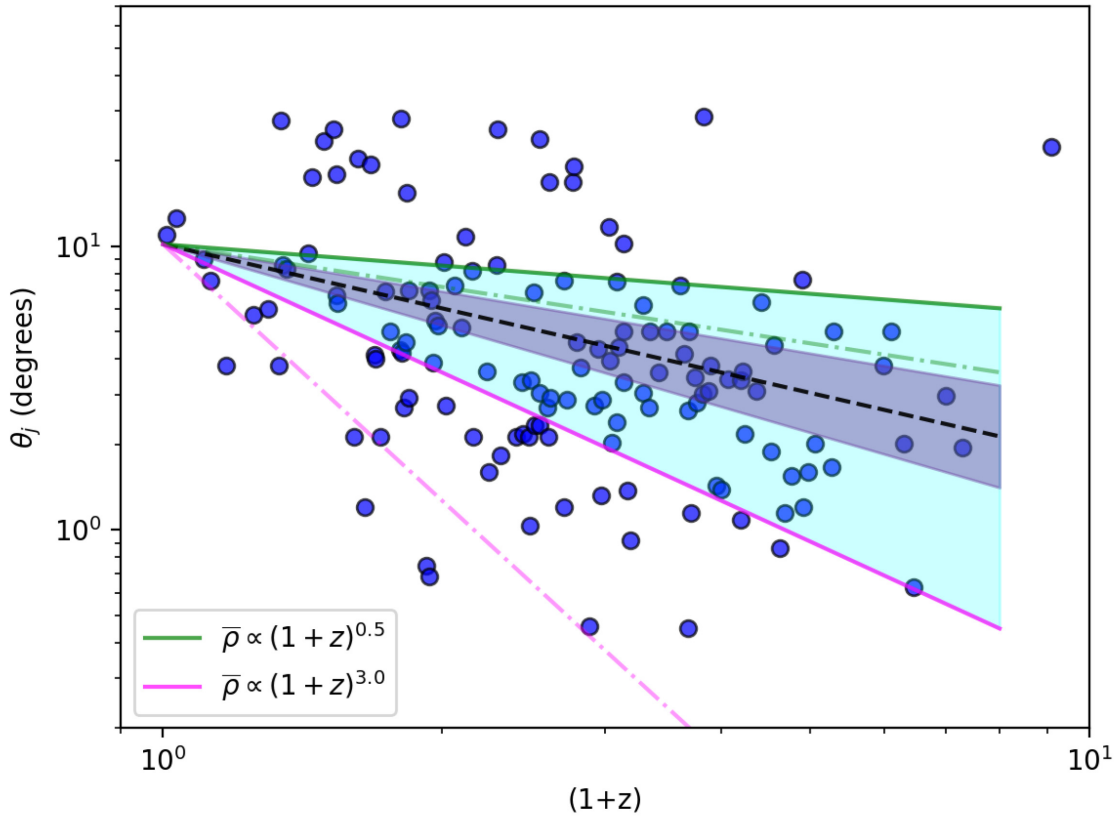

Figure 3. Jet opening angle versus redshift. The dashed black line and purple region show the best fit to the data, $\theta_j \propto (1+z)^{-0.75 \pm 0.25}$. The cyan region shows the expected relationship between θ_j and $(1+z)$ assuming that collimation of the jet is related to the average density of the star as $\theta_j \propto (1/\bar{\rho})^{1/2}$ and that the average stellar density evolves with redshift, bounded by $(1+z)^{-0.5}$ (upper green line) and $(1+z)^{3.0}$ (lower magenta line). The dash–dotted lines show the expected redshift dependence for $\theta_j \propto (1/\bar{\rho})$.

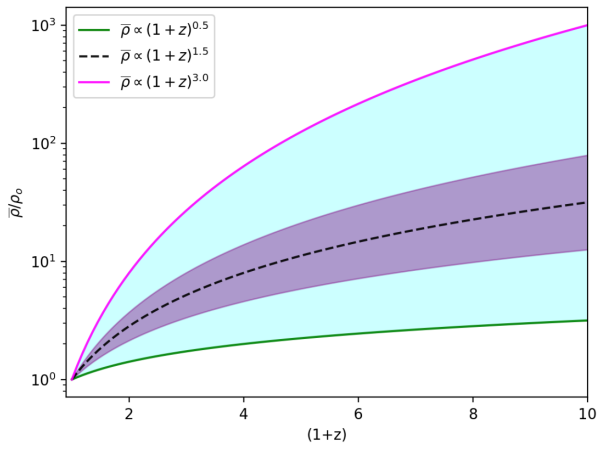

Figure 4. Models of average stellar density as a function of redshift that may contribute to the anticorrelation between jet opening angle and redshift. The dark shaded region shows the required density evolution to reproduce the best fit line to the data ($\theta_j \propto (1+z)^{-0.75 \pm 0.25}$), assuming $\theta_j \propto (1/\overline{\rho})^{1/2}$.

we expect higher mass stars to collimate the jet more. If, in addition, this density evolves with redshift according to the evolution of the characteristic mass of the IMF, then stars at higher redshift will more strongly collimate GRB jets, leading to the observed anticorrelation between jet opening angle and redshift.

Davé (2008) proposed an evolving initial stellar mass function, where the characteristic or break mass evolves according to $\tilde{m} \sim 0.5(1+z)^2\,\mathrm{M}_\odot$ (see also Davé 2011). Using equation (7) above, this would lead to a jet opening angle dependence $\theta_j \propto (1+z)^{-1}$, consistent with the observed correlation. Fig. 3 shows the jet angle–redshift relationship resulting from density (or mass) evolution ranging from $\bar{\rho} \propto (1+z)^{0.5}$ up to $\bar{\rho} \propto (1+z)^3$ (shown in Fig. 4). This of course ignores various underlying relationships between lGRB properties (and their dependence on progenitor type). For example, if higher mass stars tend to produce more luminous jets, this will mitigate the effect of the higher average stellar density collimating the jet more (although we stress again we found no correlation between L_γ and redshift). In addition the relationship between progenitor type and the underlying jet launch – intimately connected to the angular momentum and magnetic flux of the system – is also not considered. As discussed in Section 3, these issues really require high fidelity simulations of the collapse and launch of a jet under a wide range of conditions; we explore this in a future publication (Hurtado et al., in preparation).

Finally, we have assumed a weak dependence of average density on stellar radius in our discussion above. Consider the previous section which pointed out that, on average, the longer a jet spends in the stellar envelope environment the more it will be collimated. Therefore, higher radii stars (provided their envelopes are dense enough) would be expected to have more collimated jets (see Section 4.1). Stars with more mass will have somewhat larger radii and so, naively, again we are led to the conclusion that

higher mass (presumably low metallicity) stars at higher redshifts will lead to more collimated jets, consistent with the $\theta_j - (1 + z)$ anticorrelation. And indeed, if we use empirical mass–radius relationships for massive stars, $R \propto M^{\sim 0.7}$, we find that the jet opening angle depends on stellar radius as $\theta_j \propto (1/R)^{\sim 0.2 - 0.4}$. Note this is similar to the relationship between θ_j and R reported in Tchekhovskoy et al. (2010).

6 CONCLUSIONS

We have investigated the nature of the observed anticorrelation between lGRB jet opening angle and redshift. We suggest that high-redshift stars producing lGRBs have higher average density and are able to collimate a GRB jet more effectively. Higher density stars at high redshift are expected in an evolving IMF scenario, and the $\theta_j - (1 + z)$ correlation is consistent with the quantitative form of some proposed IMF characteristic mass evolution, under the assumption that average stellar density is proportional to mass for lGRB progenitors. Therefore, *we assert that beaming angle evolution is a result of progenitor mass evolution* in a collapsar scenario for lGRBs. Additionally, these higher mass stars will be slightly larger in radii (for a given metallicity) and therefore the jet will spend more time in the stellar envelope being collimated (thus emerging with a narrower opening angle). In summary:

(i) We examine the luminosity conditions for collimation and successful jet launch in a massive star progenitor and find the former is easily met, while the latter is met if we assume the gamma-ray radiative efficiency is low for some lGRBs (or, alternatively, that the stellar pressure is lower than what we have assumed). We find a strong correlation between gamma-ray luminosity and jet opening angle in the data, with $L_j \propto \theta_j^{1.5}$. We suggest this is a natural selection effect – only the most luminous GRBs are able to launch jets with wide opening angles.

(ii) Jet opening angle at breakout is inversely proportional to the average stellar density, $\theta_j \propto (1/\bar{\rho})^{\beta}$, with β between 1/2 and 1. We suggest the anticorrelation between jet opening angle and redshift can be explained if the average stellar density evolves with redshift as $\bar{\rho} \propto (1 + z)^{\sim 2 \pm 1}$. This is in line with the proposed evolution of the characteristic mass of the IMF (Davé 2008), if we can assume that density is roughly proportional to mass (i.e. has a weak dependence on radius), as has been shown for high-mass stars (Mizuta & Aloy 2009). In this case, and taking $\beta = 1/2$, we can write the jet opening angle as $\theta_j \propto (L_j/M)^{1/2}$.

We have focused on exploring the beaming angle evolution in the context of a jet propagating through a massive star envelope. We have interpreted our results in the context of average stellar density as it relates to stellar mass and radius. As discussed in Section 2.2 and throughout the paper, metallicity plays an important role in its connection to the mass and stellar structure of the lGRB progenitor. Besides the trend of a larger population of higher mass, lower metallicity stars at high redshift, Mizuta & Aloy (2009) suggest that the cocoon is more narrowly collimated in lower metallicity stars, because of the steep drop off in density outside the surface (see their fig. 1) compared to higher metallicity stars (their fig. 3). This steep drop off allows for low-metallicity jets to be more ballistic and would therefore also lead to a narrower measured jet opening angle. We again caution about the various selection effects that can complicate the determination of the lGRB jet opening angle; however, this paper provides a possible physical explanation, and to some extent a prediction of its existence in the case when the IMF is weighted toward higher mass, lower metallicity stars in the early Universe.

A very important implication of the cosmic evolution of lGRB jet opening angle is that this relationship significantly affects the rates of lGRBs as a function of redshift, with potentially many more GRBs at high redshifts than current estimates indicate. Even without accounting for beaming angle evolution, several studies (e.g. Lloyd-Ronning et al. 2002; Kistler et al. 2008; Yüksel et al. 2008; Kistler et al. 2009) suggest that the high-redshift star formation rate – under certain assumptions about its connection to the lGRB population – is higher than rates estimated from other stellar populations. Our results amplify this effect. That is, a smaller opening angle at higher redshift implies that a smaller fraction of lGRBs are observed. Thus, the lGRB rate at high redshift may be substantially underestimated in the standard models that assume a single, non-evolving jet opening angle – possibly up to an order of magnitude underestimate of the GRB rate at the highest redshifts (see fig. 7 of Hopkins & Beacom 2006 who show rate densities of core-collapse supernovae out to high redshifts for different IMFs). This also supports the suggestion that the IMF is more top-heavy at higher redshifts, as it implies a larger fraction of the total stellar mass is in massive GRB progenitor stars at higher redshift. We examine this issue in detail in an upcoming publication; future missions such as THESEUS (Amati et al. 2019), with potential to detect GRBs out to a redshift of 12, may help us test these suggestions and perhaps more definitively and ultimately determine the relationship between the GRB rate and star formation rate.

As discussed in Section 2, the anticorrelation between jet opening angle and redshift may also be explained a number of other ways for a given progenitor, including through a dependence on the amount of angular momentum retained in the star as it forms a GRB, the magnetic field strength and geometry, and/or other details of the jet launching mechanism. Additionally, we might account for the observed beaming angle evolution if different progenitor systems are be dominating the population at different redshifts – for example, Mizuta & Aloy (2009) find that collapsar jets are more narrowly beamed than jets from mergers which might indicate that collapsars are dominating the progenitor distribution at high redshift while binary scenarios dominate at low redshift (although the presence of supernovae in the light curves of long GRBs will constrain potential models and will necessitate association with a massive star in some way). The different rates of possible lGRB progenitors (e.g. table 1 of Levan et al. 2016) and their distinct signatures as a function of redshift are important questions that should be understood if we are to understand the observations of the global lGRB population (Kistler et al. 2008). We speculate that the scatter we see in the $\theta_j - (1 + z)$ correlation could be a consequence of this (different progenitors) in addition to variation among properties of single progenitor type. We explore this further in an upcoming publication.

Finally, we mention that Lloyd-Ronning et al. (2019b) also suggested there exists an anticorrelation between the intrinsic prompt duration and redshift. This trend was also seen in a radio bright subsample of energetic lGRBs, but *not* in a radio dark sample (Lloyd-Ronning et al. 2019c), hinting at the possibility of a progenitor signature/effect. Intrinsic duration of the prompt emission is a reflection of the lifetime of the disc, which in turn reflects the mass and accretion rate of the disc (although a number of external effects can affect this duration by up to a factor of two or so, e.g. Gao & Mészáros 2015). Again, all of these things relate to fundamental properties of the progenitor system, and should be understood in the context of lGRB progenitor models. As observations and simulations of these systems improve, we can

test our understanding of these trends, with the hope of learning something truly fundamental about the lGRB progenitor.

ACKNOWLEDGEMENTS

We are very grateful to the anonymous referee for valuable and helpful comments on the manuscript. We also thank Mohira Rassel, Sanjana Curtis, and Brooke Polak for enlightening discussions. This work was supported by the US Department of Energy through the Los Alamos National Laboratory. Los Alamos National Laboratory is operated by Triad National Security, LLC, for the National Nuclear Security Administration of U.S. Department of Energy (Contract No. 89233218CNA000001). JLJ and AA are supported by a LANL LDRD Exploratory Research Grant 20170317ER. LA-UR-19-31599.

REFERENCES

Abbott B. P. et al., 2017, Phys. Rev. Lett., 119, 161101
Aloy M. A., Cuesta-Martínez C., Obergaulinger M., 2018, MNRAS, 478, 3576
Amati L., O'Brien P., Gotz D., Bozzo E., 2019, in AAS/High Energy Astrophysics Division. p. 303.02
Barkov M. V., Komissarov S. S., 2008, Int. J. Mod. Phys. D, 17, 1669
Barkov M. V., Komissarov S. S., 2010, MNRAS, 401, 1644
Belczynski K., Bulik T., Rudak B., 2002, ApJ, 571, 394
Berger E., 2014, ARA&A, 52, 43
Blandford R. D., Znajek R. L., 1977, MNRAS, 179, 433
Bloom J. S., Kulkarni S. R., Djorgovski S. G., 2002, AJ, 123, 1111
Bromberg O., Nakar E., Piran T., Sari R., 2011, ApJ, 740, 100
Bromm V., Loeb A., 2006, ApJ, 642, 382
Burrows A., Dessart L., Livne E., Ott C. D., Murphy J., 2007, ApJ, 664, 416
Callingham J. R., Tuthill P. G., Pope B. J. S., Williams P. M., Crowther P. A., Edwards M., Norris B., Kedziora-Chudczer L., 2019, Nat. Astron., 3, 82
Cantiello M., Yoon S. C., Langer N., Livio M., 2007, A&A, 465, L29
Chrimes A. A., Stanway E. R., Eldridge J. J., 2020, MNRAS, 491, 3479
Chruslinska M., Jerabkova T., Nelemans G., Yan Z., 2020, A&A, 636, A10
D'Avanzo P., 2015, J. High Energy Astrophys., 7, 73
Dainotti M. G., Del Vecchio R., Tarnopolski M., 2018, Adv. Astron., 2018, 4969503
Davé R., 2008, MNRAS, 385, 147
Davé R., 2011, in Treyer M., Wyder T., Neill J., Seibert M., Lee J., eds, ASP Conf. Ser. Vol. 440, UP2010: Have Observations Revealed a Variable Upper End of the Initial Mass Function?. Astron. Soc. Pac., San Francisco, p. 353
Davies M. B., Levan A. J., Larsson J., King A. R., Fruchter A. S., 2007, in Axelsson M., Ryde F., eds, AIP Conf. Proc. Vol. 906, Gamma-Ray Bursts: Prospects for GLAST. Am. Inst. Phys., New York, p. 69
de Mink S. E., Langer N., Izzard R. G., Sana H., de Koter A., 2013, ApJ, 764, 166
Della Valle M. et al., 2006, Nature, 444, 1050
Demircan O., Kahraman G., 1991, Ap&SS, 181, 313
Deng C.-M., Wang X.-G., Guo B.-B., Lu R.-J., Wang Y.-Z., Wei J.-J., Wu X.-F., Liang E.-W., 2016, ApJ, 820, 66
Efron B., Petrosian V., 1992, ApJ, 399, 345
Fong W., Berger E., 2013, ApJ, 776, 18
Fong W., Berger E., Fox D. B., 2010, ApJ, 708, 9
Fryer C. L., Heger A., 2005, ApJ, 623, 302
Fryer C. L., Woosley S. E., 1998, ApJ, 502, L9
Fryer C. L., Belczynski K., Berger E., Thöne C., Ellinger C., Bulik T., 2013, ApJ, 764, 181
Fynbo J. P. U. et al., 2006, Nature, 444, 1047
Gal-Yam A. et al., 2006, Nature, 444, 1053
Galama T. J. et al., 1998, Nature, 395, 670
Gao H., Mészáros P., 2015, ApJ, 802, 90
Gehrels N. et al., 2006, Nature, 444, 1044
Gehrels N., Ramirez-Ruiz E., Fox D. B., 2009, ARA&A, 47, 567
Hamidani H., Kiuchi K., Ioka K., 2020, MNRAS, 491, 3192
Hjorth J., Bloom J. S., 2012, in Kouveliotou C., Wijers R. A. M. J., Woosley S., eds., Gamma-ray Bursts, Cambridge University Press, Cambridge, 169
Hjorth J. et al., 2003, Nature, 423, 847
Hopkins A. M., Beacom J. F., 2006, ApJ, 651, 142
Kelly B. C., 2007, ApJ, 665, 1489
King A., Olsson E., Davies M. B., 2007, MNRAS, 374, L34
Kinugawa T., Asano K., 2017, ApJ, 849, L29
Kistler M. D., Yüksel H., Beacom J. F., Stanek K. Z., 2008, ApJ, 673, L119
Kistler M. D., Yüksel H., Beacom J. F., Hopkins A. M., Wyithe J. S. B., 2009, ApJ, 705, L104
Kitagawa T., Nybom M., Stuhler J., 2018, Technical Report, Measurement Error and Rank Correlations, CeMMAP Working Papers. Institute for Fiscal Studies, London, UK
Kobulnicky H. A. et al., 2014, ApJS, 213, 34
Kocevski D., Liang E., 2006, ApJ, 642, 371
Komissarov S. S., Barkov M. V., 2009, MNRAS, 397, 1153
Kroupa P., 2019, preprint (arXiv:1910.06971)
Kumar P., Narayan R., Johnson J. L., 2008a, Science, 321, 376
Kumar P., Narayan R., Johnson J. L., 2008b, MNRAS, 388, 1729
Laskar T. et al., 2014, ApJ, 781, 1
Laskar T., Berger E., Chornock R., Margutti R., Fong W.-F., Zauderer B. A., 2018a, ApJ, 858, 65
Laskar T. et al., 2018b, ApJ, 859, 134
Lee W. H., Ramirez-Ruiz E., 2007, New J. Phys., 9, 17
Leja J., Speagle J. S., Johnson B. D., Conroy C., van Dokkum P., Franx M., 2020, ApJ, 893, 111
Levan A., Crowther P., de Grijs R., Langer N., Xu D., Yoon S.-C., 2016, Space Sci. Rev., 202, 33
Lloyd N. M., Petrosian V., Mallozzi R. S., 2000, ApJ, 534, 227
Lloyd-Ronning N. M., Fryer C. L., Ramirez-Ruiz E., 2002, ApJ, 574, 554
Lloyd-Ronning N. M., Fryer C., Miller J. M., Prasad N., Torres C., Martin P., 2019a, MNRAS, 485, 203
Lloyd-Ronning N. M., Aykutalp A., Johnson J. L., 2019b, MNRAS, 488, 5823
Lloyd-Ronning N. M., Gompertz B., Pe'er A., Dainotti M., Fruchter A., 2019c, ApJ, 871, 118
Lü J., Zou Y.-C., Lei W.-H., Zhang B., Wu Q., Wang D.-X., Liang E.-W., Lü H.-J., 2012, ApJ, 751, 49
Lyman J. D. et al., 2017, MNRAS, 467, 1795
Lynden-Bell D., 1971, MNRAS, 155, 95
MacFadyen A. I., Woosley S. E., 1999, ApJ, 524, 262
Mandel I., Farr W. M., Gair J. R., 2019, MNRAS, 486, 1086
Marks M., Kroupa P., Dabringhausen J., Pawlowski M. S., 2012, MNRAS, 422, 2246
Matzner C. D., 2003, MNRAS, 345, 575
Matzner C. D., McKee C. F., 1999, ApJ, 510, 379
Mészáros P., 2006, Rep. Prog. Phys., 69, 2259
Metzger B. D. et al., 2010, MNRAS, 406, 2650
Mizuta A., Aloy M. A., 2009, ApJ, 699, 1261
Mizuta A., Yamasaki T., Nagataki S., Mineshige S., 2006, ApJ, 651, 960
Morsony B. J., Lazzati D., Begelman M. C., 2007, ApJ, 665, 569
Nagakura H., Hotokezaka K., Sekiguchi Y., Shibata M., Ioka K., 2014, ApJ, 784, L28
Obergaulinger M., Aloy M. Á., 2020, MNRAS, 492, 4613
Perets H. B., Li Z., Lombardi J. C., Jr, Milcarek S. R., Jr, 2016, ApJ, 823, 113
Petrosian V., Kitanidis E., Kocevski D., 2015, ApJ, 806, 44
Piran T., 2004, Rev. Mod. Phys., 76, 1143
Press W. H., Teukolsky S. A., Vetterling W. T., Flannery B. P., 2007, Numerical Recipes 3rd Edition: The Art of Scientific Computing, 3 edn. Cambridge Univ. Press, Cambridge
Ramirez-Ruiz E., Celotti A., Rees M. J., 2002, MNRAS, 337, 1349
Rhoads J. E., 1997, ApJ, 487, L1
Rhoads J. E., 1999, ApJ, 525, 737

Rueda J. A., Ruffini R., Wang Y., 2019, Universe, 5, 110
Suwa Y., Ioka K., 2011, ApJ, 726, 107
Tanvir N. R., Levan A. J., Fruchter A. S., Hjorth J., Hounsell R. A., Wiersema K., Tunnicliffe R. L., 2013, Nature, 500, 547
Tchekhovskoy A., Narayan R., McKinney J. C., 2010, New Astron., 15, 749
Troja E. et al., 2018, Nat. Commun., 9, 4089
Tsvetkova A. et al., 2017, ApJ, 850, 161
van Dokkum P. G., van der Marel R. P., 2007, ApJ, 655, 30
Vink J. S., de Koter A., 2005, A&A, 442, 587
Vink J. S., de Koter A., Lamers H. J. G. L. M., 2001, A&A, 369, 574
Wang F. Y., Dai Z. G., 2011, ApJ, 727, L34
Wang F., Zou Y.-C., Liu F., Liao B., Liu Y., Chai Y., Xia L., 2020, ApJ, 893, 77
Wei D. M., Gao W. H., 2003, MNRAS, 345, 743
Woosley S. E., 1993, ApJ, 405, 273
Woosley S., Bloom J., 2006, ARA&A, 44, 507
Woosley S. E., Heger A., 2006, ApJ, 637, 914
Xue L., Zhang F.-W., Zhu S.-Y., 2019, ApJ, 876, 77
Yonetoku D., Murakami T., Nakamura T., Yamazaki R., Inoue A. K., Ioka K., 2004, ApJ, 609, 935
Yonetoku D., Yamazaki R., Nakamura T., Murakami T., 2005, MNRAS, 362, 1114
Yoon S.-C., Woosley S. E., Langer N., 2010, ApJ, 725, 940
Yoon S.-C., Dierks A., Langer N., 2012, A&A, 542, A113
Yu H., Wang F. Y., Dai Z. G., Cheng K. S., 2015, ApJS, 218, 13
Yüksel H., Kistler M. D., Beacom J. F., Hopkins A. M., 2008, ApJ, 683, L5
Zhang W., Fryer C. L., 2001, ApJ, 550, 357
Zhang B., Mészáros P., 2004, Int. J. Mod. Phys. A, 19, 2385
Zhang W., Woosley S. E., MacFadyen A. I., 2003, ApJ, 586, 356

This paper has been typeset from a TEX/LATEX file prepared by the author.